The 15th International Symposium on Magnetic Bearings, August 3-6, 2016, Mojiko Hotel, Kitakyushu, Japan

ISMB15

Algorithms for self-sensing magnetic bearings using current signals and least square identification

Daniel FRANZ*, Michael RICHTER* and Stephan RINDERKNECHT*

* Institute for Mechatronic Systems in Mechanical Engineering, Technische Universität Darmstadt

Otto-Berndt-Straße 2, 64287 Darmstadt, Germany

E-mail: franz@ims.tu-darmstadt.de

Abstract

This paper discusses self-sensing algorithms based on least square identification for active magnetic bearings under strong eddy current influence. The considered algorithms use current data which are acquired at high frequency to estimate the air gap size by means of the actuator inductance. Eddy currents lead to a nonlinear current increase. This can result in poor position estimation accuracy when linear approximations are used. To face this problem, two approaches are considered. In the first an exponential trial function is introduced to compensate the eddy currents. Potential problems arise, because the exponent cannot be fitted with least square identification and therefore has to be taken as constant. The other utilizes the current data of two counteracting electromagnets, which are driven asymmetrically. To compensate eddy currents as well as movement induction the signals are added up, unlike other publications where they are subtracted. The estimation algorithms are investigated with measured current data. The first reduces the error to 40 % of a reference algorithm. The second shows further improvement to 20 % of the reference. However, the error absolute values are still too high for industrial applications. The paper closes with a proposal for further improvement.

Keywords : self-sensing, active magnetic bearings, current slope, inductance, least square identification

1. Introduction

The stable operation of active magnetic bearings (AMB) requires the detection of the rotor position. In a standard AMB system this information is derived via sensors. The current increase in an AMB coil depends on its inductance and thereby on the air gap between rotor and stator. Consequently, the rotor position is inherent in the current signals. A method to extract this information, makes position sensors and their evaluation unnecessary and thereby reduces the systems cost and the complexity of the hardware. Furthermore, sensor and actuator are always collocated.

Subject of this work is the study and adaption of an algorithm to obtain the rotor position from the current signals. The aim is an acquisition of the rotor position with an accuracy of 1 µm.

2. Position estimation algorithms

Figure 1 shows a simple model of an electromagnet. The voltage u causes an electric current i through the resistance R and the coil with n turns. The current induces the magnetic flux ϕ in the ferromagnetic core. The core has an air gap x. If ϕ changes, a counteracting voltage is induced in the coil. So for the electric circuit Eq. (1) holds. Changes in ϕ can be caused by a variation in the excitation current or in the air gap. Here L_d is the differential inductance which is generally a function of i and x. With Eq. (1) it is evident that current dynamic depends on L_d and therefore on x. Consequently, it is possible to estimate the air gap x by means of measured current slop data. This is the basic idea of self-sensing in AMB. Several methods to realize this are considered in literature (Schweitzer and Maslen, 2009). This paper focuses on the digital position estimation through high frequent current measurement.

$$u = Ri + n\frac{d\phi}{dt} = Ri + L_d(x,i)\frac{di}{dt} + n\frac{\partial\phi}{\partial x}\frac{dx}{dt} \quad \text{with} \quad L_d(x,i) = n\frac{\partial\phi}{\partial i} \tag{1}$$

Most AMB systems use switching power amplifier which, when a two-level pulse-width modulation (PWM) is used, continuously changes the applied coil voltage from $+u$ to $-u$ during the time t_{pwm}. The voltage switching leads to a high frequent current increase and decrease. Recent algorithms use the slope of this current ripple to estimate the inductance of the AMB and thereby its air gap (e.g.: (Glueck, et al., 2011), (Wang and Binder, 2014)). In this paper the relation $x = x(L_d, i)$ will be represented by a measured lookup table.

In most AMB systems two opposing magnets are used for one axis. The switching in one actuator induces a current peak in the other actuator. To reduce this source of error for the position estimation, the actuators are driven asymmetrically. When a positive voltage is applied to one actuator, the other is applied with a negative voltage. In common differential driving mode when the current is increased in one actuator, it is decreased in the counteracting actuator. So for the asymmetric drive the middle switching is more or less simultaneous in both actuators (Fig. 2). Because the actuators have separate current control, the middle switching point can differ, if the inductance is unequal, e.g. when the rotor is eccentric. Hence, for a high rotor eccentricity it is possible that the current samples around the middle switching point have to be neglected in the position estimation. However, no switching peak should occur in the middle of a current edge.

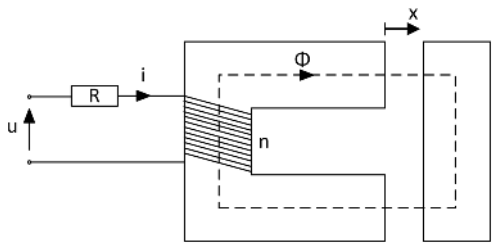

Fig. 1 Model of the magnetic actuator.

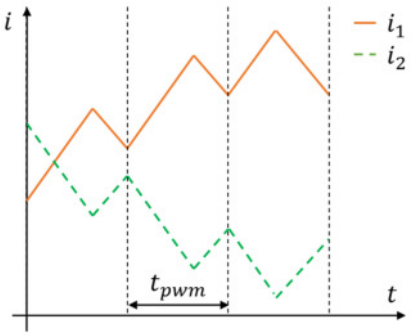

Fig. 2 Excitation currents in two counteracting magnets.

2.1. Linear approximation

If the current alteration can be approximated as linear the, inductance can the estimated via a least square fit of a linear trial function to the current data during a pulse-width. This is implemented in the direct digital inductance estimation (DDIE) (Glueck, et al., 2011). Here the fitted inductances of the rising and the falling edge during t_{pwm} are aggregated to reduce the influence of the rotor movement and changes of the coil resistance. However, measurements with low-grade core materials show strong nonlinear coil current alteration (Fig. 3). Mostly this can be attributed to eddy currents induced by the flux change during switching (Richter, et al., 2014). This nonlinearity appears as the main source of inaccuracy concerning the position estimation of the DDIE. After the switching the flux alteration is nearly constant and thereby the induced eddy currents are as well. Therefore, the excitation current tends to a constant increase. The point where the current can be seen as linear depends on the material properties of the core. Including the nonlinear area in a linear estimation leads to a duty cycle dependent outcome. This is due to the different estimated current slops when the pulse-width differs, even when the real current behavior stays the same. This is illustrated in Fig. 3. The dashed line shows the linear fit for a pulse-width of 15 µs, whereas the solid line shows the linear fit for a pulse-with of 25 µs, both for the same measured current data. A different approach would be to acquire a fixed number m of samples at m fixed time steps after the switching for the slop calculation, because eddy current behavior, and therefore the nonlinear coil current increase, is expected to be independent of the pulse-width. To restrict the current dynamic as little as possible, m and the time steps should be chosen small, making slope calculation very susceptible to noise. However, excluding the nonlinear area from the estimation reduces the system dynamics. This is attributed to the minimum pulse-width which has to be defined to make sure that the linear region is long enough for the estimation. To avoid loss of dynamics, the aim of this work is to integrate the nonlinearity in the estimation algorithm.

2.2. Nonlinear approximation

To increase the estimation accuracy the linear function can be replaced by a nonlinear function $\tilde{\imath}$. The differential

inductance in the period $[t_0, t_1]$ can be approximated with:

$$\mathrm{L_d} \approx \frac{\int_{t_0}^{t_1}(u - R\tilde{\imath})\ dt}{\tilde{\imath}(t_1) - \tilde{\imath}(t_0)} = n\frac{\Delta\tilde{\Phi}}{\Delta\tilde{\imath}} \tag{2}$$

where $t_{pwm} \gg (t_1 - t_0) \neq 0$. To account for the nonlinearity of $\tilde{\imath}$, t_1 and t_0 each have to be selected in equal distance to the switching point for every pulse-width, but they do not necessarily have to correspond to the measured data. For the fit of $\tilde{\imath}$ all available current samples of one pulse-width can be used. This makes this approach less susceptible to noise. For $\tilde{\imath}$ a polynomial of higher order, for example cubic (Eq. (3)), could be used.

$$\tilde{\imath} = at^3 + bt^2 + ct + d \tag{3}$$

This would consider nonlinearity but would not compensate it (Fig. 4), what results from the poor extrapolation behavior of polynomials. The estimation still depends on the duty cycle. The aim of the trial function should be to extrapolate the measured current data to its linear region. After the switching the eddy current change decays exponentially. Accordingly, an exponential term is added to a linear trial function (Eq. (4)).

$$\tilde{\imath} = \tilde{\imath}_{lin} - ae^{-bt} = ct + d - ae^{-bt} \tag{4}$$

The exponent b cannot be fitted with least square identification and a nonlinear algorithm would be to slow for an online position estimation. So the exponent has to be taken as constant and is fitted offline. When the current samples are synchronized with switching, the expression e^{-bt_i} stays the same for every pulse-width and can be provided for the calculation as a constant vector $[1 \quad \cdots \quad e^{-ibt_{samp}} \quad \cdots \quad e^{-mbt_{samp}}]$, where t_{samp} is the sampling period and m is the number of measured samples during t_{pwm}. However, for this paper a constant sampling frequency was used and so the measurements are not synchronized with switching. The resulting change in b is expected to be small and is neglected. To increase the evaluation speed it is possible to estimate the position directly via the linear slope coefficient c, instead of calculating the inductance, as all essential measured information is inherent in c.

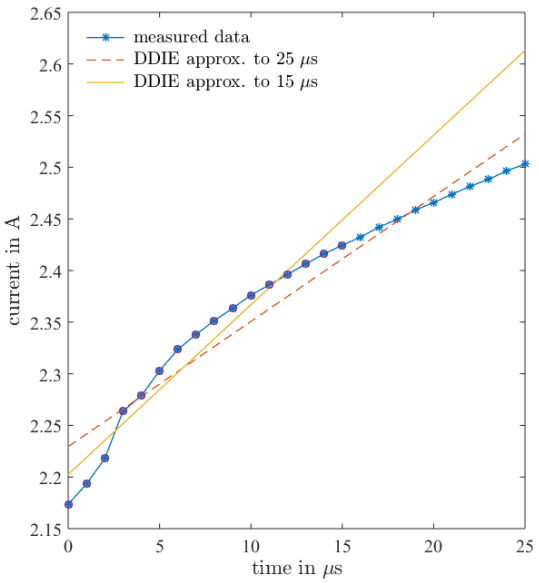

Fig. 3 Comparison of the estimated current slop of a pulswidth of 15 µs and 25 µs.

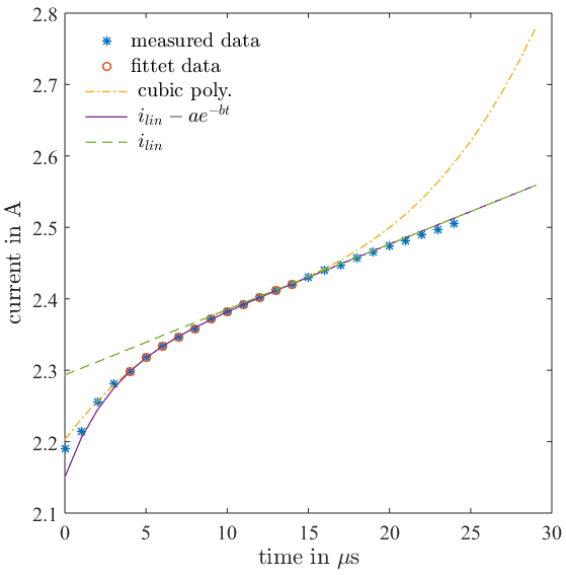

Fig. 4 Comparison of the extrapolation behavior of a cubic polynomial and an exponential trial function as current approximations

2.3. Current sum

A third approach utilizes the current data of both opposing magnets in one axis. The sum of both current deviations, each derived from Eq. (1), yields Eq. (5). Here it is beneficial that the magnets are driven asymmetrically (Fig. 2). The resulting flux change is always contrary and so is the influence of the eddy currents. In the current sum the eddy currents are mostly compensated and the sum alteration is nearly linear.

$$\frac{di_1}{dt}+\frac{di_2}{dt}=\frac{di_m}{dt}=u\frac{L_{d2}-L_{d1}}{L_{d1}\ L_{d2}}-\frac{R_1 i_1}{L_{d1}}-\frac{R_2 i_2}{L_{d2}}+n\left(L_{d2}^{-1}\frac{\partial\phi_2}{\partial x}-L_{d1}^{-1}\frac{\partial\phi_1}{\partial x}\right)\frac{dx}{dt} \tag{5}$$

The voltage induced by the rotor movement in both actuators is inverse. When the current signals of the opposing actuators are added up, the movement induced currents cancel each other partially out. For the differential inductance Eq. (6) holds (see appendix). Hence the velocity dependent expression in Eq. (5) can be transformed to Eq. (7). The influence of the rotor movement on the current sum dynamic is proportional to the difference between the flux in both actuators. Consequently, the movement influence vanishes around the centered position.

$$\frac{\partial\phi}{\partial x}=-\frac{2\phi}{n^2\mu_0 A}L_d \tag{6}$$

$$n\left(L_{d2}^{-1}\frac{\partial\phi_2}{\partial x}-L_{d1}^{-1}\frac{\partial\phi_1}{\partial x}\right)\frac{dx}{dt}=\frac{2}{n\mu_0 A}(\phi_1-\phi_2)\frac{dx}{dt} \tag{7}$$

In Fig. 5 the currents in both actuators (left) and their sum (right) at a stationary eccentricity of 0.5 mm with a nominal air gap of 1 mm are shown. The measured current signals are added digitally. The current control leads to slightly different switching point in both coils. This results in a short peak in the current sum which is excluded from the estimation, yet the linear region is reached much faster than the signal of a single coil. This problem could be avoided when the current sampling is synchronized with the voltage switching in each actuator, which is only possible for a digital summation.

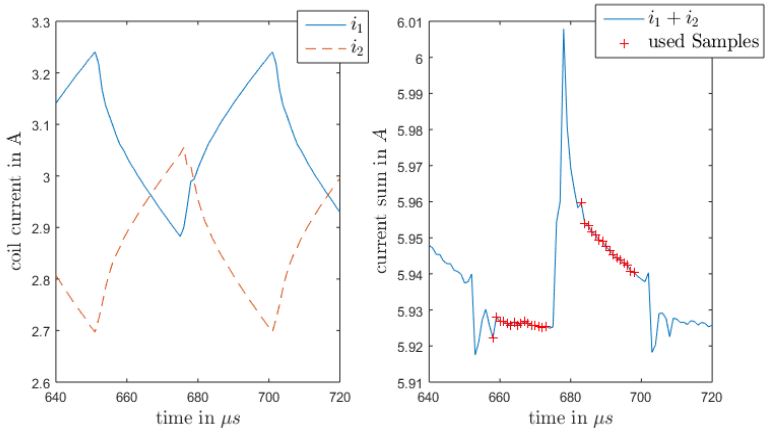

Fig. 5 left: both coil currents; right: current sum

3. Experimental investigation

To investigate aforementioned methods, measurements on a uniaxial test rig with two counteracting electromagnets using differential driving mode were performed. The test rig is shown in Fig. 6. The stator is located in the middle, while the surrounding frame is movable in the actuator direction and fixed in the other two directions with wires. The actuators are composed of low-grade 0.35 mm M165-35S silicon steel sheets, which develop strong eddy currents. Each coil has 145 turns. On the right a laser triangulation sensor is located to measure the frame position as reverence. The PWM frequency is 20 kHz and the current is sampled with 1 MHz, thus at most 50 Samples are recordable during t_{pwm}.

At first the current is measured at several stationary rotor positions and various constant set currents. With this information, a look-up table was created for the rotor position depending on the mean current and estimated inductance. The algorithms were tested offline, with a measured sinusoidal changing set current with a frequency of 125 Hz and an amplitude of 1 A around the bias of 3 A at a stationary rotor eccentricity of 0.2 mm towards the right actuator B. No rotor movement is investigated in this paper.

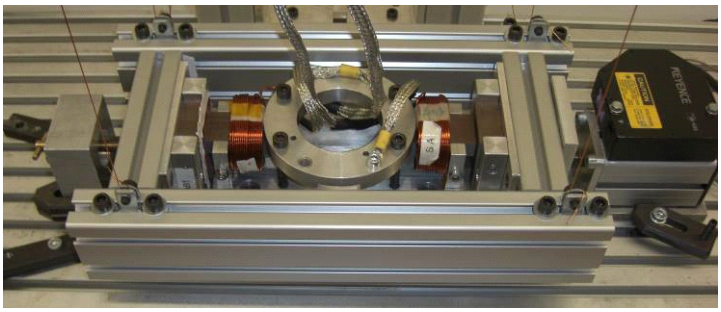

Fig. 6 uniaxial test rig

In the experiments the DDIE shows huge estimation errors up to 250 µm (Fig. 8), although the first twelve strongly nonlinear samples of every current edge where neglected. The error curve repeats with the current change, hence it can mostly be attributed to a systematic error. Noise leads to a standard deviation of approximately 10 µm. For the exponential trial function (Eq. (4)) the measurements reveal a strong influence of the coil current and the air gap on the fitted exponent. Nevertheless, the estimated positon using a constant exponent shows a reduced error. With 100 µm the maximum error is 40 % of the DDIE (Fig. 9). This can partially be traced back to the weighting characteristic of the exponential function. The influence of the first, strongly nonlinear current samples on the estimation is reduced. Consequently, a short pulse-width leads to an unreliable estimation, if the exponent doesn't correspond to the real decay behavior. The standard deviation with 10,5 µm is slightly higher than in the DDIE. Figure 10 shows the error curve for the current sum method. Here the first seven samples of every current edge where neglected. The maximum error is below 50 µm and thus 20 % of the DDIE. The standard deviation with 6,8 µm is smaller than the others.

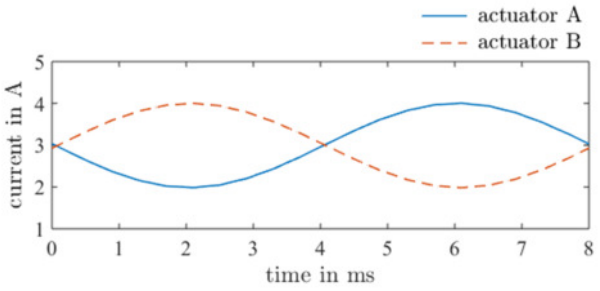

Fig. 7 In the test the coil currents where varied with 125 Hz and an amplitude of 1 A around the bias of 3A.

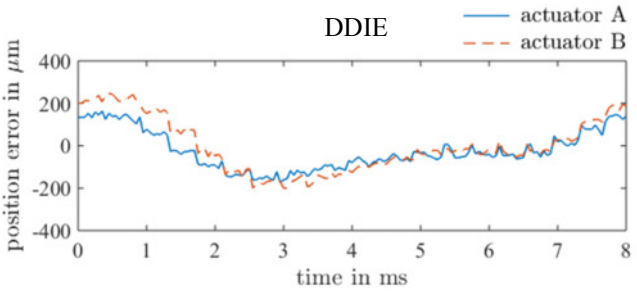

Fig. 8 Error in the estimated position using DDIE with a nominal air gap of 1 mm and a eccentricity of 0.2 mm.

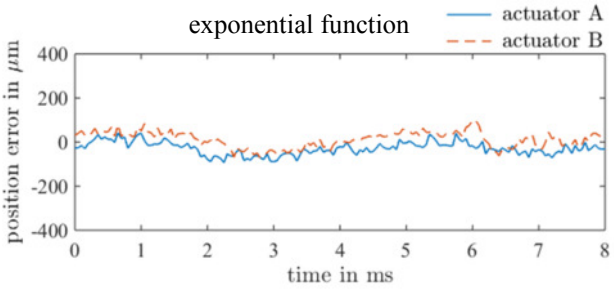

Fig. 9 Error in the estimated position using the exponential trial function Eq. (4) with a nominal air gap of 1 mm and a eccentricity of 0.2 mm.

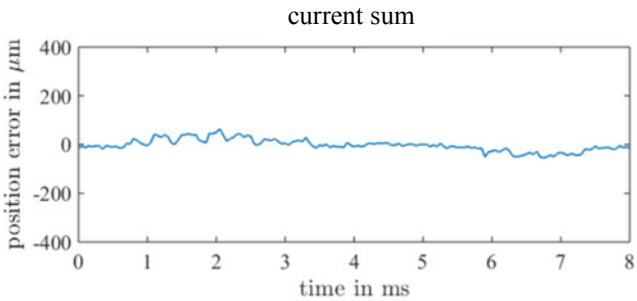

Fig. 10 Error in the estimated position using the current sum with a nominal air gap of 1 mm and a eccentricity of 0.2 mm.

4. Conclusion and Outlook

Using low-grade core materials in AMB results in a nonlinear increase of the current edge after voltage switching. This leads to high position estimation errors when a linear trial function is used. The error can be reduced in case that the eddy current influence is considered by an exponential trial function. The exponent cannot be fitted online leading to inaccuracy when the pulse-with is short or the sampling is not synchronized with the PWM. In the sum of the current signals of two counteracting magnets the movement induction and eddy currents are partially compensated for asymmetrically driven magnets. This approach reduces the estimation error to 20 % of the reference algorithm DDIE. Nevertheless, the desired accuracy of 1 µm could not be reached. The error is still too high for industrial applications and thus further improvements are necessary.

A higher accuracy is expected for all considered methods if the current sampling is synchronized with voltage switching so that the sampling always takes place at same time during a current edge.

For the fit of the exponential function the exponent b was assumed to be constant, whereas the measurements reveal a dependency of b on the coil current. In Fig. 11 b is shown as a function of the current, separately evaluated for the rising and falling edge of a pulse-width. Every mark at a fixed current stands for a different air gap between 0,5 mm and 1,5 mm. For the rising edge b increases nearly linear with the current, while it decreases for the falling edge. This proportionality can be implemented in the estimation to adjust b and thereby increase the estimation accuracy.

One Problem of the last algorithm is that it uses the signals of the AMB current sensors which have a measuring range of a few amperes while the current change during a duty cycle is just a few mA. The current sum always has an offset of two times the bias which leads to poor resolution of the current change. To remove the offset it is possible to measure the current sum using a summing transformer (Fig. 12), analog to the differential transformer used in (Matsuda et al., 1996) or (Nenning et al., 2014). Only the high frequent current changes induce a voltage u_3 in the secondary coil. The induced voltage can directly be used for the position estimation and no curve fitting is necessary. Further, for small rotor displacements the current sum compensates the rotor movement and eddy currents.

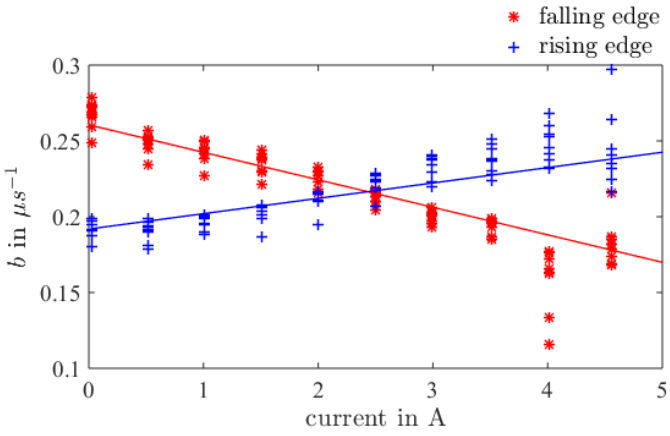

Fig. 11 The fitted exponent b of the rising current edge increases with the mean current, while it decreases for the falling current edge. At every mean current the exponent is displayed for various air gaps.

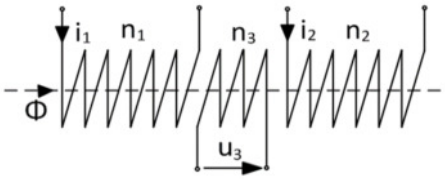

Fig. 12 summing transformer

Appendix

In the actuator shown in Fig. 1, the supplied electric energy W_{el} and the external mechanical energy W_{mech} is converted into magnetic energy W_{mag}. Therefore Eq. (8) holds (Kallenbach, et al., 2012).

$$\underbrace{\int n\frac{\partial\phi}{\partial t}i\ dt}_{W_{el}} + \underbrace{\int F\ dx}_{W_{mech}} = \underbrace{\int ni\ d\phi}_{W_{mag}} \tag{8}$$

where $\phi = \phi(x,i)$ and $F = F(x,i)$. i and x are independent variables and are assumed to be constant. Hence, Eq. (8) can be transformed to Eq. (9).

$$n\phi i + \int F\ dx = n\phi i - n\int \phi\ di \tag{9}$$

The derivate of Eq. (9) with respect to i and x leads to Eq. (10). For the actuator from Fig. 1 the derivate of F with respect to ϕ can be calculated with Eq. (11) (Kallenbach, et al., 2012).

$$-n\frac{\partial\phi}{\partial x} = \frac{\partial F}{\partial i} = \frac{\partial F}{\partial\phi}\frac{\partial\phi}{\partial i} = \frac{L_d}{n}\frac{\partial F}{\partial\phi} \tag{10}$$

$$\frac{\partial F}{\partial\phi} = \frac{2\phi}{\mu_0 A} \tag{11}$$

Consequently, the derivate of ϕ with respect to x can be obtained from the differential inductance and the flux from:

$$\frac{\partial\phi}{\partial x} = -\frac{2\phi}{n^2\mu_0 A}L_d. \tag{12}$$

References

Glueck, T., Kemmetmueller, W., Tump, C., und Kugi, A., A novel robust position estimator for self-sensing magnetic levitation systems based on least squares identification, Control Engineering Practice., vol. 19, no. 2, (2011), pp. 146–157.

Nenning, T., Hofer, M., Hutterer, M., Schrödl, M., Setup with two self-sensing magnetic bearings using differential 3-Active INFORM, Proceedings of the 14th International Symposium on Magnetic Bearings, (2014), pp. 689-692.

Kallenbach, E., Eick, R., Quendt, P., Ströhla, T., Feindt, K., Kallenbach, M., Elektromagnets, Vieweg+Teubner Verlag, (2012). pp. 45-69 (in German)

Matsuda, K., Okada, Y., Tani, J., Self-sensing magnetic bearing using the principle of differential transformer, Proceedings of the 5th International Symposium on Magnetic Bearings, (1996), pp. 107-112.

Richter, M., Schaede, H., Rinderknecht, S., Investigations on the “direct digital inductance estimation”-concept for self-sensing AMBs under influence of eddy currents, Proceedings of the 14th International Symposium on Magnetic Bearings, (2014), pp. 693-698.

Schweitzer, G. and Maslen, E.H., Magnetic bearings, Springer, (2009), pp. 435-459.

Wang, J. and Binder, A., Position Estimation for Self-Sensing Magnetic Bearings Based on Double Detection of Current Slopes, Proceedings of the 14th International Symposium on Magnetic Bearings, (2014), pp. 673-678.